Articles

Structure and Biosynthesis of Hectoramide B, a Linear Depsipeptide from Marine Cyanobacterium *Moorena producens* JHB Discovered via Coculture with *Candida albicans*

Thuan-Ethan Ngo, Andrew Ecker, Byeol Ryu, Aurora Guild, Ariana Remmel, Paul D. Boudreau, Kelsey L. Alexander, C. Benjamin Naman, Evgenia Glukhov, Nicole E. Avalon, Vikram V. Shende, Lamar Thomas, Samira Dahesh, Victor Nizet, Lena Gerwick, and William H. Gerwick*

Cite This: https://doi.org/10.1021/acschembio.3c00391
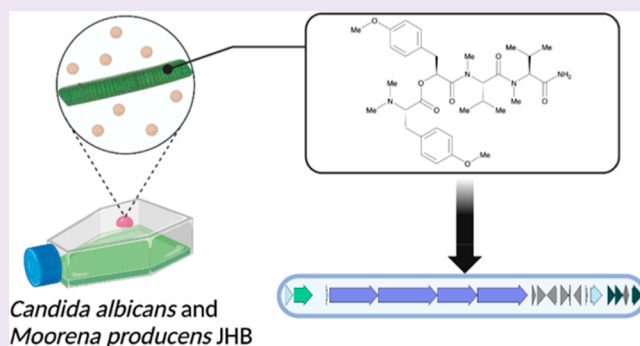
Read Online

ACCESS | Metrics & More | Article Recommendations | SI Supporting Information

ABSTRACT: The tropical marine cyanobacterium *Moorena producens* JHB is a prolific source of secondary metabolites with potential biomedical utility. Previous studies on this strain led to the discovery of several novel compounds such as hectochlorins and jamaicamides. However, bioinformatic analyses of its genome indicate the presence of numerous cryptic biosynthetic gene clusters that have yet to be characterized. To potentially stimulate the production of novel compounds from this strain, it was cocultured with *Candida albicans*. From this experiment, we observed the increased production of a new compound that we characterize here as hectoramide B. Bioinformatic analysis of the *M. producens* JHB genome enabled the identification of a putative biosynthetic gene cluster responsible for hectoramide B biosynthesis. This work demonstrates that coculture competition experiments can be a valuable method to facilitate the discovery of novel natural products from cyanobacteria.

Candida albicans and *Moorena producens* JHB

INTRODUCTION

Members of cyanobacterial genus *Moorena* are tropical, filamentous, photosynthetic, nondiazotropic and generally inhabit the marine benthic zone.[1] Notably, they serve as a prolific source of bioactive secondary metabolites. For instance, apratoxin A, a cyclic depsipeptide isolated from *Moorena bouillonii* collected in Guam, is a potent inhibitor of protein synthesis.[2–4] Comparative genomics of species of this genus has revealed their extensive biosynthetic potential, with ∼18% of their genomes dedicated to secondary metabolism. Notably, the average number of biosynthetic gene clusters (BGCs) in these species is generally much higher than other cyanobacteria.[5] Intriguingly, a significant number of these BGCs remain silent or cryptic, and are yet to be explored for their encoded products. Therefore, new approaches are needed to induce or enhance the production levels of these natural products.

Tropical filamentous marine cyanobacterium *Moorena producens* JHB, formerly known as *Lyngbya majuscula* (hereinafter referred to as JHB), was obtained from a shallow marine environment in Hector's Bay, Jamaica. It has been continuously cultivated in seawater-BG11 (SWBG11) culture medium since its original collection.[6] This cyanobacterium is an abundant producer of diverse bioactive secondary metabolites, including the potent antifungal NP hectochlorins A–D,[6]

sodium channel antagonists jamaicamides A–F,[7,8] cryptomaldamide,[9] and hectoramide A (Figure 1).[7] Although numerous compounds have been isolated from a single cyanobacterium, genome analysis revealed the existence of as many as 42 cryptic gene clusters yet to be investigated, 11 of which contain nonribosomal peptide synthetase (NRPS)-related genes.[5] Therefore, we sought to drive the expression of some of these previously uninvestigated BGCs through stimulation by a competing microorganism, *Candida albicans*—a method well known to upregulate the expression of NPs.[10,11]

RESULTS AND DISCUSSION

Discovery from Coculture Experiment. The biomass from both co- and monocultures of JHB with and without *C. albicans* was harvested, extracted, and analyzed in triplicate by LCMS after 4 weeks of incubation. The peak areas of metabolites observed by LCMS were compared to identify
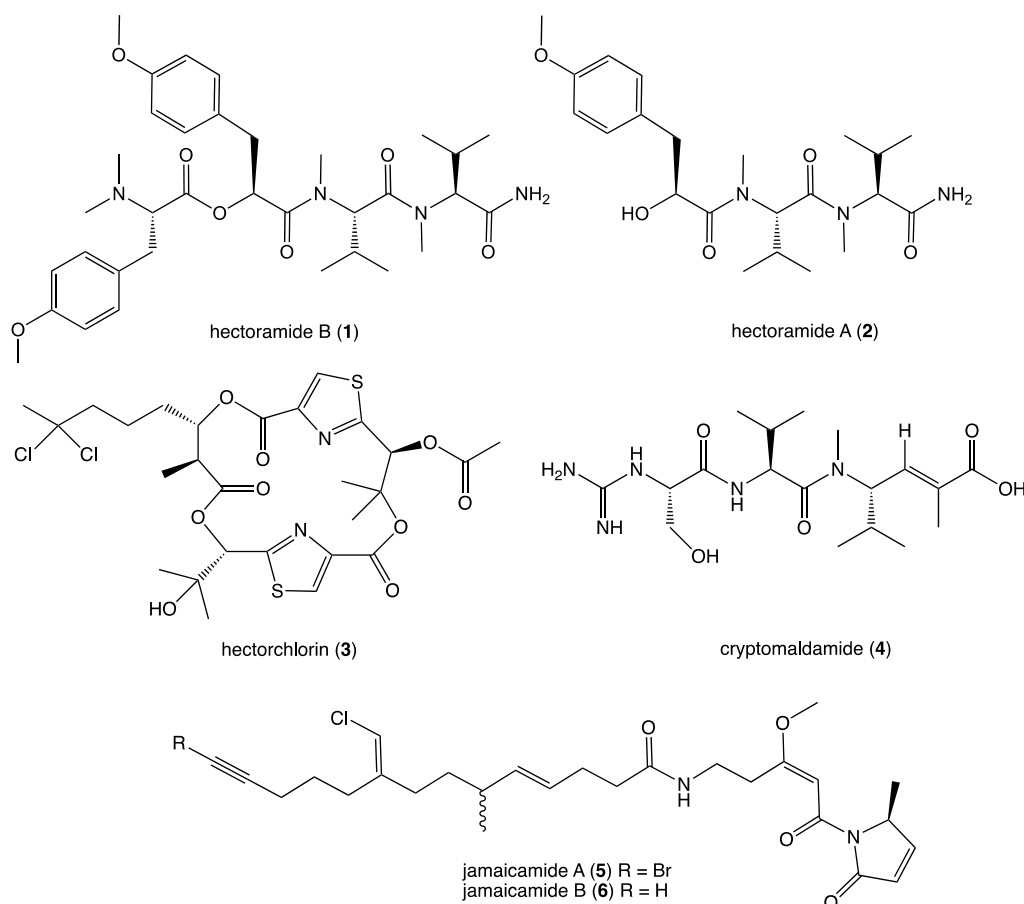
A

Figure 1. Natural products isolated and characterized from *Moorena producens* JHB.

metabolites exhibiting enhanced production in coculture experiments compared to the controls. We observed that the cocultures had an antagonistic effect on the growth of the cyanobacteria, with biomass of cocultured cyanobacteria greatly reduced compared to the monocultures after the same growth period. Notably, the production of hectoramide B (1) in the coculture with JHB and *C. albicans* appeared increased relative to the monoculture of JHB (Figure S14). This possible metabolic upregulation inspired interest in identifying and characterizing the structure, BGC, and bioactivity of this unique metabolite.

Structure Determination of Hectoramide B (1). Hectoramide B (1) was initially isolated by VLC and high-performance liquid chromatography (HPLC), yielding 1.7 mg of yellow oil from the coculture experiments. Based on HRMS (obsd [M + H] m/z 627.3750; calcd 627.3757), a putative molecular formula for compound 1 was calculated as $C_{34}H_{50}N_4O_7$. The 12 degrees of unsaturation required for this molecular formula were deduced through the interpretation of nuclear magnetic resonance (NMR) data, indicating the presence of two phenyl rings and four ester/amide-type carbonyls.

The ^{1}H NMR spectrum of compound 1 was remarkably similar to that of the previously determined structure of hectoramide,[7] here renamed hectoramide A (2). Moreover, analysis of the MS/MS fragmentation using GNPS molecular networking[12] also revealed the close relationship between 1 and 2. However, the larger size of 1 suggested the possible presence of an additional amino acid residue compared to 2.

Additional NMR signals in 1, not present in 2, included aromatic proton peaks, N- and O-methyl singlets, and a deshielded proton alpha to a heteroatom coupled to a midfield methylene group. These findings together suggested that this additional amino acid might be an N,N-dimethyl-O-methyl tyrosine moiety.

SMART-NMR[13] analysis of the HSQC spectrum of 1 further suggested the presence of multiple valine residues as well as methylated tyrosine residues (Figure S7). HSQC, HMBC, and COSY correlations confirmed the sections of compound 1 that were identical to compound 2 and also established the new residue as the proposed trimethyl-tyrosine residue (Figure 2a).

This observation was further supported by the analysis and comparison of the MS/MS fragmentation for 2 and 1, revealing some shared MS^2 peaks (Figure 2b). Previous determination of the absolute configuration of 2,[7] combined with a bioinformatic analysis as detailed below, was used to infer the absolute configuration of 1. These analyses allowed deduction of the configurations of the tyrosine and both valine derivatives as L and the MPPA moiety as S.

BGC Analysis. Nonribosomal peptides are typically synthesized in a collinear manner, wherein each module encodes for the incorporation of an amino or hydroxy acid residue, and chain elongation occurs in the sequence dictated by the order of the modules.[14]

A retrobiosynthetic scheme for the probable hectoramide B BGC was developed based on its chemical structure, including modules consistent with a NRPS incorporation of amino or
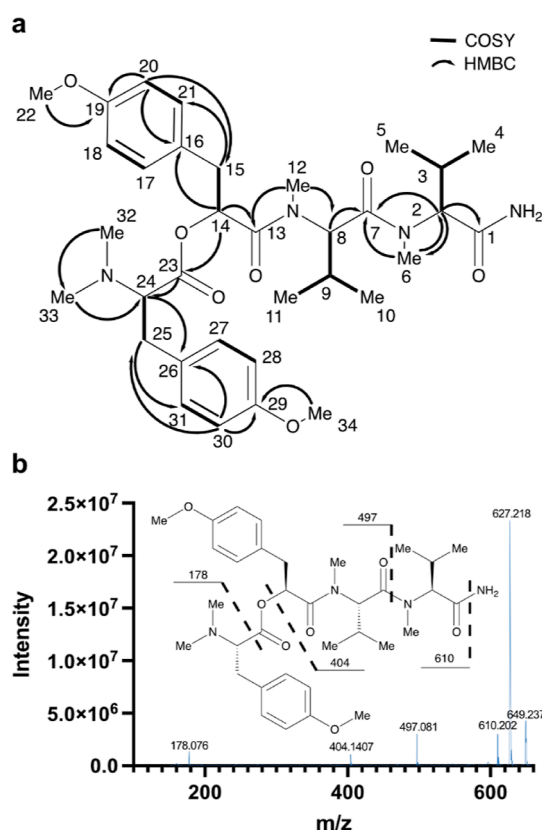
a

b

Figure 2. Structural assignment of hectoramide B. (a) Key COSY and HMBC correlations used in the structural determination of hectoramide B (**1**). All of the COSY and HMBC correlations are reported in Table S1. (b) Fragmentation pattern of **1** based on the MS^2 spectrum from the molecular ion (m/z 627.218).

genome (Table 1). The final assembly of the JHB genome resulted in a single circular scaffold of 9.6 Mbp, a GC content

Table 1. Evaluation of the Quality of Genome Assembly Based on Quast and BUSCO[a] Analysis

assembly method	#of contigs	N50	total length (bp)	complete[a] (%)
SPades	3	9,373,345	9,384,763	98.84
unicycler long-read	2	8,738,093	9,632,771	60.67
unicycler hybrid	2	5,885,695	9,639,251	99.22
flye	1	9,645,659	9,645,659	79.56
flye + pilon	1	9,648,534	9,648,534	99.22

[a]Completeness was based on the presence of complete single copy orthologs in the BUSCO cyanobacteria_odb10 database.

of 43.67%, and a completeness of 99.22%. Therefore, we selected this assembly for BGC analysis using antiSMASH (GenBank Accession Number: CP017708.2).

Putative BGC for Hectoramide B. Inspection of the *M. producens* JHB genome revealed one candidate BGC that was consistent with the biosynthesis of hectoramide B (the *hca* pathway; MiBIG Accession: BGC0002754, GenBank Accession: OQ821997), the predicted retrobiosynthetic scheme, and the NMR- and MS-based structural assignment of hectoramide B (**1**) (Figure S8 and Table S9). AntiSMASH annotations were integrated with protein family homology analysis, substrate selectivity predictions, and active site and motif identification. The *hca* pathway is flanked by putative regulatory genes, transport-related genes, and coding regions for hypothetical proteins, providing provisional boundaries to the biosynthetic cluster (Figure 3).

Bioinformatic analysis of the *hca* gene cluster suggested that the initial core biosynthetic module, *hcaA*, encodes a multienzyme that is responsible for incorporating a tyrosine residue. This module contains condensation (C), adenylation (A), O-MT (OMT), and NMT domains, as well as a peptidyl carrier protein (PCP) domain. The presence of both an OMT and the NMT is consistent with the amino terminus structure of hectoramide B. However, initial AntiSMASH analysis predicted the presence of two NMT domains, and therefore, a phylogenetic tree of OMT and NMT domains from cyanobacteria was generated to examine more carefully the specificities of each of the annotated MT domains in *hcaA*. This revealed that the first MT, HcaA-MT1, clades well with other OMT domains, such as the OMT in the VatN module of the vatiamide BGC[15] (Figure S10). The vatiamide OMT is also predicted to methylate the phenolic oxygen atom of a tyrosine residue. The second MT, HcaA-MT2, clades well with other NMT domains, specifically those within the *hca* pathway and the NMT of the VatN module in the vatiamide pathway. Therefore, *N,N*-dimethyl-*O*-methyl-L-tyrosine serves as the first structural unit in the *hca* pathway.

The second module, *hcaB*, is predicted to encode a protein that ultimately incorporates 2-hydroxy-3-(4-methoxyphenyl)-propanoic acid (MPPA). In previous studies of cyanobacterial depsipeptide formation, the A domain initially selects for an α-keto acid substrate that is reduced *in cis* to an α-hydroxy acid by a KR domain before incorporation into the natural product scaffold.[12] However, antiSMASH analysis of this module did not reach a consensus for substrate specificity, and there was no annotation for an OMT domain to install a methyl group

hydroxy acids, and tailoring enzymes for key structural modifications such as methyl groups on heteroatoms (Figure S8). We hypothesized that the initial module would be an NRPS that would contain an adenylation (A) domain specific for tyrosine incorporation, followed by methyltransferase (MT) domains that would catalyze the methylations of the tyrosine phenolic oxygen atom and the nitrogen atom of the amine group. We predicted that module 2 would include a depsipeptide synthetase that would incorporate an α-keto acid version of tyrosine that is subsequently reduced to 2-hydroxy-3-(4-hydroxyphenyl) propanoic acid by a ketoreductase (KR) domain. This module should also include a MT domain that methylates the phenolic oxygen atom of this tyrosine-derived residue. Modules 3 and 4 are predicted to contain A domains that incorporate valine residues, followed by methylation by an *N*-MT (NMT). A terminal amidation enzyme is predicted to be encoded at the distal end of module 4, possibly related to the one observed in carmabin A[10] and vatiamide E and F[11] biosynthesis, completing the pathway.

Previous sequencing efforts of the JHB genome utilized Illumina MiSeq and were assembled using a *M. producens* PAL reference assembly.[5] However, upon the initial inspection of this assembly, we were unable to identify a candidate BGC. Therefore, we sought to obtain an improved genome assembly of JHB by extracting high-molecular-weight DNA and obtaining long reads with Nanopore PromethION sequencing. Previous sequencing data from Illumina MiSeq and the new sequencing data from Nanopore PromethION were assembled with different tools to obtain an improved assembly of the JHB
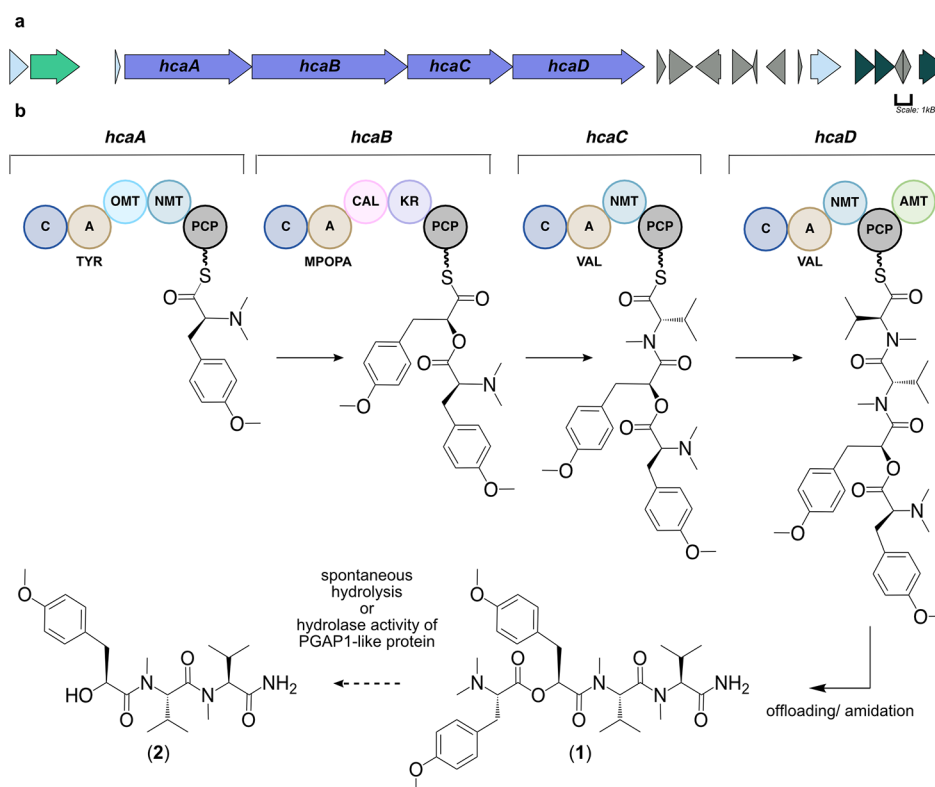
Figure 3. Putative BGC for hectoramide B. (a) Purple arrows indicate the core biosynthetic genes. Additional arrows indicate additional ORFs that provide provisional boundaries to the hca BGC. Their proposed functions can be found in Table S9. (b) There are four core biosynthetic modules organized in a colinear fashion in the hca pathway. C: condensation domain; A, adenylation domain; TYR, adenylation domain for tyrosine incorporation; OMT: oxygen methyltransferase domain; NMT: nitrogen methyl transferase domain; MPOPA: adenylation domain for the proposed MPOPA incorporation; CAL: coenzyme A ligase domain; KR: ketoreductase domain; VAL: adenylation domain for valine incorporation; and AMT: amidotransferase. PCP: peptidyl-carrier protein. Phosphopantetheine arms are symbolized by wavy lines associated with four core biosynthetic NRPS modules (hcaA-hcaD).

on the phenolic oxygen atom. Therefore, a sequence and structural alignment of the HcaB-A domain with other NRPS A domains selected for tyrosine and phenylalanine was generated to identify the specificity conferring residues of hcaB-A (Figure 4a). Interestingly, the proposed specificity conferring residues of HcaB-A did not coincide with previous patterns observed in α-keto acid selecting A domains. Typically, in keto-acid activating A domains, the conserved Asp235 residue, which traditionally hydrogen-bonds with the primary amine of amino acids, is substituted with an aliphatic residue, while the remaining specificity-conferring residues match those predicted for the corresponding amino acid.[16] However, neither was the case for HcaB-A; Asp235 is still present, and the remaining proposed specificity conferring residues did not match those expected for tyrosine (Figure 4a). Furthermore, alignment of a predicted structural model constructed *de novo* with AlphaFold2[17] of HcaB-A and crystallography-derived structures of other NRPS A domains showed excellent congruence with the specificity conferring codes suggested by the sequence alignment described above (Figure 4b). Finally, as noted, there was no annotated OMT domain in the *hcaB* gene. One possibility that is consistent with these features is that hcaB could be selecting for the α-keto acid form of *O*-methyl-tyrosine, 3-(4-methoxyphenyl)-2-oxopropanoic acid (MPOPA), rather than the α-keto acid form of tyrosine. An additional methyl group on the phenolic oxygen atom would require a significant alteration of the

specificity binding pocket in order to accommodate this bulkier side chain.

α-Keto acids can also be selected for by an antiparallel carbonyl–carbonyl interaction between the α-keto group and the carbonyl of the peptide bond connecting Gly414 and Met415.[18] This carbonyl–carbonyl interaction has a strength comparable to that of a hydrogen bond and is important to α-keto acid selection. However, based on the model of HcaB-A (Figure 4b), the only residue that is in close proximity to the α-keto group is Asp235 (3.0 Å), whereas the Gly–Met backbone carbonyl is far distant. The predicted antiparallel orientation of these two carbonyls suggests a basis for stabilizing the incorporation of this α-keto acid.

Another component of this module is the domain annotated as a coenzyme A ligase (CAL). CAL domains are predicted to have specificity for fatty acids; however, as there are no fatty acid moieties in hectoramide B, it may be nonfunctional. Interestingly, similar CAL domains are found in a number of other depsipeptide producing BGCs such as cryptophycin-327,[19] hectochlorin,[20] and didemnin B[21] and therefore could be playing another role in the production of depsipeptides, a hypothesis that warrants further investigation. Last, the KR domain in the HcaB module is predicted to have stereo-specificity for an S product. We propose that after activation of MPOPA, the KR domain in this module reduces the α-keto acid to 2S-hydroxy-3-(4-methoxyphenyl)propanoic acid (MPPA) through an NADPH-dependent reaction. The C-domain then catalyzes the formation of the ester bond between
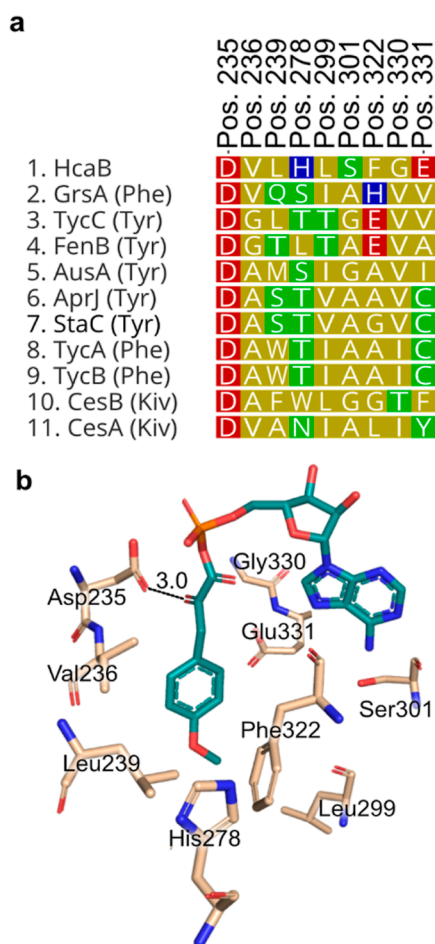
a

1. HcaB   D V L H L S F G E
2. GrsA (Phe) D V Q S I A H
3. TycC (Tyr) D G L T T G E V V
4. FenB (Tyr) D G T L T A E V A
5. AusA (Tyr) D A M S I G A V I
6. AprJ (Tyr) D A S T V A A V C
7. StaC (Tyr) D A S T V A G V C
8. TycA (Phe) D A W T I A A I C
9. TycB (Phe) D A W T I A A I C
10. CesB (Kiv) D A F W L G G T F
11. CesA (Kiv) D V A N I A L I Y

b

Figure 4. Sequence and structural alignment of the hcaB adenylation domain reveal amino acids potentially conferring specificity. (a) Putative specificity conferring codes of the HcaB-A domain compared with those from other adenylation domains from NRPS systems. See Figure S11 for compound identities and other information. (b) Three-dimensional model of the HcaB-A domain generated using Alphafold2 bound to MPOPA adenylate. The α-keto group of MPOPA (teal) potentially binds through an antiparallel carbonyl–carbonyl interaction with the side chain carbonyl group of Asp235 (wheat).

the oxygen of the newly formed hydroxy function in this module 2 substrate and the carbonyl of the tethered trimethyl tyrosine residue in module 1.

Based on annotation by antiSMASH, HcaC is predicted to encode the incorporation of an *N*-methyl valine into hectoramide B. The final module, HcaD, is also predicted to incorporate an *N*-methyl valine residue. However, it lacks a terminal thioesterase domain; instead, it possesses a domain closely related (83.5% identity, Table 2 and Figure S13) to that found in the vatiamide pathway that is believed to catalyze offloading from the enzymatic pathway through terminal amidation. In the vatiamide pathway, this proposed enzymatic function is embedded in VatR, downstream of the PCP; the same domain organization is observed in the hectoramide B pathway.[15] Terminal amides resulting from an NRPS pathway have previously been found in several cyanobacterial natural products, including dragonamide A, B, and E;[22] carmabin A;[23] and vatiamide E and F.[15] Although the mechanism and enzymology of terminal amidation have not been studied, it is hypothesized that this motif catalyzes offloading through

Table 2. Sequence Identity and Similarity between Terminating Modules HcaD and VatR

amino acid position	predicted function	identity/similarity
76−380	condensation	23.0/43.0
555−952	adenylation	88.2/95.0
1046−1267	NMT	90.1/95.0
1477−1543	PCP	83.6/91.0
1544−1977	amidotransferase	83.5/93.0
	overall	72.0/86.7

ammonolysis, mechanistically similar to the more typical hydrolysis of NRPS thioester linkages.

In addition to the core domains in the *hca* gene cluster, an upstream regulatory gene, ORF 2, was identified (Table S9). This regulatory gene belongs to the Streptomyces Antibiotic Regulatory Protein family, a group of transcriptional regulators commonly found in actinomycetes that regulate the biosynthesis of various antibiotic gene clusters.[24,25] This discovery suggests that ORF 2 may play a pivotal role in controlling the production of hectoramide B. However, further analysis and investigation are necessary to fully understand its specific involvement and mechanism of action within the *hca* gene cluster. A PGAP1-like protein with hydrolase activity in ester bonds was identified in ORF1 and may also play a role in the biosynthesis of hectoramide A. It is plausible that after the offloading of **1**, ORF1 catalyzes the hydrolysis of the ester bond in **1**, ultimately leading to the formation of **2**.

Exploring the Bioactivity of Hectoramide B. To explore the potential antifungal properties of hectoramide B (**1**), microbroth dilution methods were employed. The original strain of *C. albicans* used in the coculture experiments was no longer available, which prevented repeat testing with this strain. We therefore evaluated the activity of hectoramide B against two well-characterized prototype strains of *Candida* (*C. albicans* and *Candida auris*) as well as to *Saccharomyces cerevisiae*. However, no antifungal activity was detected at a maximum test concentration of 128 μg/mL of hectoramide B against the two *Candida* species nor 200 μg/mL against the *Saccharomyces* strain. Given the lack of meaningful antifungal activity, the underlying reason for its increased production in the coculture experiment with *Candida* remains unknown.

■ CONCLUSIONS

Genome sequencing projects of marine cyanobacteria have revealed that they, like many other bacteria, contain a large number of orphan gene clusters that encode cryptic natural products. Antagonistic coculture experiments have been successful in stimulating the expression of some of these natural product BGCs,[10] and we were interested to explore this concept with our marine cyanobacterial cultures. We found hectoramide B to be prominently upregulated in the coculture experiment with *C. albicans*. The structure of hectoramide B (**1**) was determined from a careful analysis of its spectroscopic features, comparison to the cometabolite hectoramide A (**2**), and a bioinformatic investigation of its BGC. Although direct anti-*Candida* activity was not detected for hectoramide B (**1**), it is still possible that hectoramide B plays a role in protecting *M. producens* JHB from antagonism by *C. albicans*. The *hca* gene cluster and its encoded protein components show several interesting features, such as an unusual motif for α-hydroxy acid incorporation, the presence of CAL in depsipeptide formation, and pathway termination through a putative

ammonolysis reaction. Further biochemical interrogation of the formation of these C-terminal amides is certainly warranted. This terminal amide moiety is a popular bioisostere for improving cellular permeability of carboxylic acids;[26] understanding how marine cyanobacteria produce this structural feature may enable development of biocatalytic methods for its creation.

METHODS

General Considerations. Optical rotation was measured on a Jasco P-2000 polarimeter using a 1 cm microcell (JASCO International Co. Ltd., Tokyo, Japan). UV and IR spectra were recorded on Beckman Coulter DU-800 (Beckman Coulter Life Sciences, Indianapolis, USA) and Nicolet iS50 FT-IR spectrometers (Thermo Fisher Scientific, Inc.), respectively. NMR spectra were recorded by using a JEOL ECZ 500 MHz NMR spectrometer (Akishima, Tokyo, Japan). Data for NMR spectra are reported as follows: shift (δ) in ppm; s, singlet; d, doublet; t, triplet; q, quartet; m, multiplet or unresolved; brs, broad signal; and J, coupling constant (s) in Hz. NMR spectra were analyzed using MestreNova version 14.3.0−30573 (Mestrelab, Santiago de Compostela, Spain). Mass spectrometry data were analyzed using Xcalibur Qual Browser v. 1.4 SR1 (Thermo Fisher Scientific, Inc.). LR-LCMS data were collected on a Thermo Finnigan Surveyor Autosampler/LC-Pump-Plus/PDA-Plus instrument with a Thermo Finnigan Advantage Max mass spectrometer. HPLC purification was carried out with a Thermo Scientific Dionex Ultimate 3000 Pump/RS/Autosampler/RS Diode Array Detector/Automated Fraction Collector using Chromeleon software. An Agilent 6230 time-of-flight mass spectrometer (TOFMS) with a Jet Stream electrospray ionization source (ESI) was used for high-resolution mass spectrometry (HR-MS) analysis. The Jet Stream ESI source was operated under positive ion mode with the following parameters: VCap: 3500 V; fragmentor voltage: 160 V; nozzle voltage: 500 V; drying gas temperature: 325 °C; sheath gas temperature: 325 °C; drying gas flow rate: 7.0 L/Min; sheath gas flow rate: 10 L/Min; and nebulizer pressure: 40 psi. Solvents used for extraction, purification, and LC−MS/MS analyses were purchased from Fisher Chemical. All solvents were of HPLC grade except H_2O which was purified with a Millipore Milli-Q system before use. Deuterated solvents were purchased from Cambridge Isotope Laboratories.

Microbial Strains and Culture Conditions. As previously reported, *M. producens* JHB was collected from Hector's Bay, Jamaica, on August 22, 1996. The JHB culture has been continuously maintained in SWBG11 media in our laboratory at 26 °C with a 16 h light/8 h dark regimen[6] since its original collection. *C. albicans* and *S. cerevisiae* were stored in a −80 °C freezer in LB media with 20% glycerol and obtained from ATCC.

Growth of *C. albicans* in SWBG11 Media. LB media and SWBG11 media were prepared separately according to standard protocols.[27] Five combinations of LB-SWBG11 media were prepared at the following ratios of LB/SWBG11:60:40%, 40:60, 20:80, 10:90, and 100% LB media to determine the optimal ratio for growth of *C. albicans* in SWBG11 media. Each media type (30 mL) was aliquoted into a 50 mL Falcon tube. 1 mL of *C. albicans* seed culture in LB media (1 mL) was added to each tube and incubated for 24 h at 37 °C. Each combination was prepared in triplicate. A small amount of *C. albicans* growth was clearly observed in the lowest ratio of 10:90 LB-SWBG11 media, and this condition was used for subsequent coculture experiments.

Coculture of Cyanobacteria with *C. albicans*. Cyanobacteria were grown for 4 weeks in SWBG11 artificial seawater growth medium at 27 °C and 756 Lux in triplicate, with the following combinations: *M. producens* JHB alone and *M. producens* JHB + *C. albicans*. This light intensity was chosen because it was consistent with conditions that JHB culture was accustomed to in order to minimize changes to variables that might affect growth and productivity. Samples of *M. producens* JHB were prepared separately and added to 125 mL of SWBG11 medium in a sterile 250 mL plastic bottle. These bottles were inoculated with 5 mL of *C. albicans* from the LB-

SWBG11 medium prepared above. Similarly, JHB in 125 mL of SWBG11 medium was prepared as controls. The bottles were sealed and opened and gently aerated with swirling motion in a biosafety cabinet to facilitate adequate gas exchange.

Extraction and LC−MS of Co- and Monocultures. After the co- and monocultures were incubated for 30 days, the biomass was harvested from each sample through vacuum filtration. Each culture sample was extracted four times using 2:1 dichloromethane/methanol (DCM/MeOH) by sonication for 3 min, followed by soaking for 15−20 min to obtain crude extracts. Each crude extract was diluted to a concentration between 0.5 and 4 mg mL^{-1} (Table S14). A 1 mg portion of the extract was subjected to filtration using a C18 SPE column, dried under N_2, and redissolved in LC−MS grade MeOH for a final concentration of 1 mg mL^{-1}. The samples of the extract and a blank of MeOH were analyzed by LR-LCMS using a Phenomenex Kinetex 5 μm C18 100 A 100 × 4.60 mm column at a flow rate of 0.6 mL/min. The mobile phase was composed of solvent A, water +0.1% formic acid (FA), and solvent B, acetonitrile (ACN). A 32 min method was used starting with equilibration at 30% solvent B in solvent A for 2 min, followed by a linear 22 min gradient to 99% solvent B, followed by a 4 min washout phase at 99% solvent B, and a 4 min re-equilibration period at 30% solvent B in solvent A. Data-dependent acquisition of MS/MS spectra was performed in the positive ion mode.

Extraction and LC−MS of Hectoramide B (1). A fresh laboratory culture sample of *M. producens* JHB was harvested through vacuum filtration, resulting in 492.28 g of biomass (wet weight). It was extracted four times using 2:1 DCM/MeOH by sonication for 3 min, followed by soaking for 15−20 min to afford 8.82 g of extract. A 1 mg portion of the extract was subjected to filtration using a C18 SPE column, dried under N_2, and redissolved in LC−MS grade MeOH for a final concentration of 1 mg mL^{-1}. The samples of the extract and a blank of MeOH were subjected to LCMS and HR-MS analysis as described above.

VLC and HPLC Purification. A 4.05 g portion of the crude extract was dissolved in 4 mL of 2:1 DCM/MeOH and mixed in a 500 mL round-bottom flask with 16.2 g of thin-layer chromatography grade silica. The mixture was dried and loaded onto a 400 mL column for liquid chromatography (VLC). Fixed 300 mL volumes of hexanes, EtOAc, and MeOH solvents were used that progressively increased in polarity: (A) 100% hexanes, (B) 10% EtOAc/hexanes, (C) 20% EtOAc/hexanes, (D) 40% EtOAc/hexanes, (E) 60% EtOAc/hexanes, (F) 80% EtOAc/hexanes, (G)100% EtOAc, (H) 25% MeOH/EtOAc, and (I) 100% MeOH. Fractions H and I contained hectoramide B (1) and were combined and solubilized in 100 mL of EtOAc for liquid−liquid extraction with H_2O. Three iterations of liquid−liquid extraction were performed in a separatory funnel to remove salts, giving an organic layer of 0.5253 g for combined fractions H + I. Fractions H + I were purified by HPLC using a Thermo Scientific Dionex Ultimate 3000 Pump/RS/Autosampler/RS Diode Array Detector/Automated Fraction Collector that yielded six subfractions. A Phenomenex Kinetex 5 μm C18 100 Å LC 150 mm × 21.2 mm column was used for reversed-phase separation at a flow rate of 9 mL/min. The mobile phase consisted of solvent A, water +0.1% FA, and solvent B, 100% ACN. A 32 min method was used starting with equilibration at 20% solvent B in solvent A for 5 min, followed by a linear 20 min gradient to 99% solvent B, followed by a 3 min washout phase at 99% solvent B, and a 4 min re-equilibration period at 20% solvent B in solvent A. The third subfraction from this separation of fractions H + I contained compound 1 and was purified further by HPLC using a Phenomenex Kinetex 5 μm C18 100 Å LC 100 × 4.60 mm column at a flow rate of 1 mL/min and gradient elution as described above. This purification procedure from the monoculture of *M. producens* JHB afforded 16.5 mg of 1.

Hectoramide B (1). Pure hectoramide A (1) was a yellow oil; $[\alpha]_D^{25}$ −74 (c 1.0, CH_2Cl_2); UV (MeOH) λ_{max} (log ε) 225 (4.03), 275 (3.23) nm; IR (ATR) ν_{max} 3340, 2962, 2931, 2873, 1726, 1612, 1514, 1466, 1388, 1356, 1302, 1248, 1204, 1178, 1032 cm^{-1}; ^1H and ^{13}C NMR data, see Table S1; LRESIMS obs. $[M + H]^+$ m/z 627 (100),

610 (11), 497 (5), 404 (4), 178 (4); HRESIMS obs. $[M + H]^+$ m/z 627.3750 (calcd for $C_{34}H_{51}N_4O_7$, 627.3752).

DNA Extraction, Nanopore Sequencing of *M. producens* JHB, and Hybrid Assembly. DNA extraction was performed using a QIAGEN Bacterial Genomic DNA (gDNA) Extraction Kit using the standard kit protocol. The quality of the gDNA was evaluated by Nanodrop, 1% agarose gel electrophoresis, and Qubit.

Data generation was conducted using the Oxford Nanopore PromethION sequencing platform by UC Davis Genomics Core. SQK-LSK110 and FLO-PRO002 were used for library construction and data generation. All data generation was conducted using the manufacturer's protocols. Base-calling used Guppy v5.0.7 with the dna_r9.4.1_450bps_hac model. A subset of the sequencing read data was generated with Filtlong v.0.2.1[28] with parameters Min_length = 2000, keep-percent = 90, and target_bases = 1,500,000,000 for read filtering.

Two long-read assembly tools (Unicycler v.0.5.0[29] and Flye v.2.9),[30] which can conduct assembly using only Nanopore reads or with the addition of Illumina reads, were used for this study. Flye was used for assembly using only Nanopore reads with genome-size = 9 m as a parameter. Unicycler was used for assembly using only Nanopore reads and in combination with Illumina reads with default parameters for hybrid assembly and long-read only assembly. Unicycler utilizes SPades, Racon, and Pilon as part of the workflow. Metagenome binning was conducted using Metabat2 v2.15.[31] The bins were annotated using CheckM v.1.2.0[32] with taxonomy workflow, rank = phylum, and taxon = Cyanobacteria as the parameters. Bins that contained assemblies with ~43% GC content and a total contig length of ~9 Mbp were selected for genome polishing by Pilon.

Short reads from a previous Illumina sequencing effort were mapped to the assembly using bwa-mem2 v.0.7.17,[33] and polishing was conducted using Pilon v.1.24[34] with default parameters. Three iterations of polishing were performed. The genome is deposited in Genbank with accession number CP017708.2.

For polished genome evaluation, BUSCO v.5.3.2[35] was used with the cyanobacteria_odb10 database. N50, number of contigs, and genome lengths were identified using Quast v.5.0.2[36] with default parameters. To assess BGC content, AntiSMASH v.6.0[37] was used on the web-based platform with settings detection = relaxed, and all extra features enabled. The resulting region that contained the putative hectoramide B BGC was downloaded as a GenBank file and investigated further using Geneious Prime v.2022.1.1.

Sequence Alignments and Phylogenetic Tree. Sequence alignments were generated using Clustal Omega v.1.2.3 on Geneious Prime software with the default parameters. MT domain and adenylation domain sequences were obtained from the NCBI and MiBIG databases.[38] The phylogenetic tree was generated using a Geneious Tree Builder with the Jukes-Cantor model and default parameters. The MT domains used in the phylogenetic tree generation are listed in Table 1 of the Supporting Information. An oxygen MT from *Tistrella mobiliz* KA091029−065 was used as the outgroup. Sequence alignment figures were generated by EsPript 3.0.[39]

Structural Model and Alignment. The model of the hcaB adenylation domain was built using AlphaFold2[17] with the ligand being placed by aligning to other known A domains in MOE[40] using the standard parameters in the AMBER14 force field. The model was then solvated with a 10 Å sphere of water. The solvated ligand placement was refined using a steepest descent energy minimization method, followed by 10 ns of low mode molecular dynamics to confirm the binding conformations of the side chains. The simulation began with 10 ps of equilibration at 0 K, followed by a 100 ps thermal equilibration from 0 to 300 K. The simulation then underwent 100 ps of thermal bath equilibration at 300 K before the production ran. Productions were run for 10 ns with a time step of 0.5 fs to not overshoot bond vibrations. This final model was analyzed in PyMol v.2.0.[41] The model was superimposed onto other adenylation domains (A-domains) from the PDB database to obtain structural alignments (Table S12). The A-domain residues within 5 Å of the binding pocket

ligand in the hcaB model were evaluated as potential binding site residues by comparison with the other A-domains.

Biological Assays. Minimum inhibitory concentrations (MICs) to the two *Candida* species were determined following the guidelines of the European Committee on Antimicrobial Susceptibility Testing (EUCAST).[42] *C. auris* AR390 and *C. albicans* AR761 strains were grown in Yeast Peptone Dextrose overnight at 30 °C with shaking. The inoculum was prepared according to EUCAST methods with modifications as follows: RPMI 1640 (US Biological R8998−07) was supplemented with 2% glucose and buffered with morpholinepropanesulfonic acid adjusted to pH 7.0. Hectoramide B (**1**) was serially diluted in a 96-well plate and added at a final starting concentration of 128 μg/mL. After 24 h, the absorbance was read at 530 nm using an Enspire Alpha plate reader (PerkinElmer).

MIC to the *S. cerevisiae* ABC16-Monster strain were determined using microtiter broth dilution in Yeast Peptone Dextrose (YPD) media. Frozen spore suspensions of *S. cerevisiae* were grown on an overnight plate culture in YPD agar. Wells were inoculated to a final concentration of 1.5×10^5 cfu/mL. Well plates were incubated at 30 °C for 20 h, and the MICs were defined as the lowest concentration of drug completely inhibiting visible growth. Cycloheximide and fluconazole were used as positive controls.

■ ASSOCIATED CONTENT

ⓢ Supporting Information

The Supporting Information is available free of charge at https://pubs.acs.org/doi/10.1021/acschembio.3c00391.

NMR and other spectroscopic data and spectra for hectoramide B, additional analysis of the biosynthetic gene cluster for hectoramide B production, data from the LC−MS analysis of the preliminary coculture and monoculture experiments, and data generated from evaluation of hectoramide A for anti-*Candida* activity (PDF)

■ AUTHOR INFORMATION

Corresponding Author

William H. Gerwick − *Center for Marine Biotechnology and Biomedicine, Scripps Institution of Oceanography, University of California San Diego, La Jolla, California 92093, United States; Skaggs School of Pharmacy and Pharmaceutical Sciences, University of California San Diego, La Jolla, California 92093, United States;* ⓞ orcid.org/0000-0003-1403-4458; Email: wgerwick@health.ucsd.edu

Authors

Thuan-Ethan Ngo − *Center for Marine Biotechnology and Biomedicine, Scripps Institution of Oceanography, University of California San Diego, La Jolla, California 92093, United States;* ⓞ orcid.org/0009-0004-7566-9208

Andrew Ecker − *Center for Marine Biotechnology and Biomedicine, Scripps Institution of Oceanography, University of California San Diego, La Jolla, California 92093, United States; Department of Pharmaceutical Chemistry, Cardiovascular Research Institute, University of California San Francisco, San Francisco, California 94143, United States;* ⓞ orcid.org/0000-0001-7331-0825

Byeol Ryu − *Center for Marine Biotechnology and Biomedicine, Scripps Institution of Oceanography, University of California San Diego, La Jolla, California 92093, United States;* ⓞ orcid.org/0000-0002-3405-2875

Aurora Guild − *Center for Marine Biotechnology and Biomedicine, Scripps Institution of Oceanography, University of California San Diego, La Jolla, California 92093, United States*

Ariana Remmel − *Center for Marine Biotechnology and Biomedicine, Scripps Institution of Oceanography, University of California San Diego, La Jolla, California 92093, United States*

Paul D. Boudreau − *Center for Marine Biotechnology and Biomedicine, Scripps Institution of Oceanography, University of California San Diego, La Jolla, California 92093, United States; Department of BioMolecular Sciences,, University of Mississippi, School of Pharmacy, University, Mississippi 38677, United States;* orcid.org/0000-0001-5416-4404

Kelsey L. Alexander − *Center for Marine Biotechnology and Biomedicine, Scripps Institution of Oceanography, University of California San Diego, La Jolla, California 92093, United States; Department of Chemistry, University of California San Diego, La Jolla, California 92093, United States;* orcid.org/0000-0002-4727-5349

C. Benjamin Naman − *Center for Marine Biotechnology and Biomedicine, Scripps Institution of Oceanography, University of California San Diego, La Jolla, California 92093, United States; Department of Science and Conservation, San Diego Botanic Garden, Encinitas, California 92024, United States;* orcid.org/0000-0002-4361-506X

Evgenia Glukhov − *Center for Marine Biotechnology and Biomedicine, Scripps Institution of Oceanography, University of California San Diego, La Jolla, California 92093, United States*

Nicole E. Avalon − *Center for Marine Biotechnology and Biomedicine, Scripps Institution of Oceanography, University of California San Diego, La Jolla, California 92093, United States;* orcid.org/0000-0003-3588-892X

Vikram V. Shende − *Center for Marine Biotechnology and Biomedicine, Scripps Institution of Oceanography, University of California San Diego, La Jolla, California 92093, United States;* orcid.org/0000-0001-8396-6297

Lamar Thomas − *Department of Pediatrics, University of California, San Diego, La Jolla, California 92093, United States;* orcid.org/0000-0003-4751-8029

Samira Dahesh − *Department of Pediatrics, University of California, San Diego, La Jolla, California 92093, United States;* orcid.org/0009-0006-4451-2034

Victor Nizet − *Department of Pediatrics, University of California, San Diego, La Jolla, California 92093, United States; Skaggs School of Pharmacy and Pharmaceutical Sciences, University of California San Diego, La Jolla, California 92093, United States;* orcid.org/0000-0003-3847-0422

Lena Gerwick − *Center for Marine Biotechnology and Biomedicine, Scripps Institution of Oceanography, University of California San Diego, La Jolla, California 92093, United States;* orcid.org/0000-0001-6108-9000

Complete contact information is available at:
https://pubs.acs.org/10.1021/acschembio.3c00391

Author Contributions

The manuscript was written through contributions of all authors. All authors have given approval to the final version of the manuscript.

Funding

Notes

The authors declare no competing financial interest.

■ ACKNOWLEDGMENTS

■ ABBREVIATIONS

A, adenylation; ACN, acetonitrile; AMT, amidotransferase; BGC, biosynthetic gene cluster; C, condensation; CAL, coenzyme A ligase; COSY, correlated spectroscopy; DCM, dichloromethane; EtOAc, ethyl acetate; FA, formic acid; gDNA, genomic DNA; GNPS, global natural products social molecular networking; HMBC, heteronuclear multiple bond correlation; HPLC, high-performance liquid chromatography; HSQC, heteronuclear single-quantum coherence; JHB, *Moorena producens* JHB; KR, *ketoreductase*; LC−MS, liquid chromatography mass spectrometry; MeOH, methanol; MIC, minimum inhibitory concentration; Mpopa, 3-(4-methoxyphenyl)-2-oxopropanoic acid; MPPA, 2-hydroxy-3-(4-methoxyphenyl)propanoic acid; MT, methyltransferase; NMR, nuclear magnetic resonance; NMT, nitrogen-methyltransferase; NRP, nonribosomal peptide; NRPS, nonribosomal peptide synthetase; OMT, oxygen-methyltransferase; PCP, peptidyl-carrier protein; SARP, streptomyces antibiotic regulatory protein; TE, thioesterase; VLC, vacuum liquid chromatography

■ REFERENCES

(1) Engene, N.; Rottacker, E. C.; Kaštovský, J.; Byrum, T.; Choi, H.; Ellisman, M. H.; Komárek, J.; Gerwick, W. H. Moorea Producens Gen. Nov., Sp. Nov. and Moorea Bouillonii Comb. Nov., Tropical Marine Cyanobacteria Rich in Bioactive Secondary Metabolites. *Int. J. Syst. Evol. Microbiol.* **2012**, *62* (Pt_5), 1171−1178.

(2) Liu, Y.; Law, B. K.; Luesch, H. Apratoxin A Reversibly Inhibits the Secretory Pathway by Preventing Cotranslational Translocation. *Mol. Pharmacol.* **2009**, *76* (1), 91−104.

(3) Luesch, H.; Yoshida, W. Y.; Moore, R. E.; Paul, V. J.; Corbett, T. H. Total Structure Determination of Apratoxin A, a Potent Novel Cytotoxin from the Marine Cyanobacterium Lyngbya majuscula. *J. Am. Chem. Soc.* **2001**, *123* (23), 5418−5423.

(4) Paatero, A. O.; Kellosalo, J.; Dunyak, B. M.; Almaliti, J.; Gestwicki, J. E.; Gerwick, W. H.; Taunton, J.; Paavilainen, V. O. Apratoxin Kills Cells by Direct Blockade of the Sec61 Protein Translocation Channel. *Cell Chem. Biol.* **2016**, *23* (5), 561−566.

(5) Leao, T.; Castelão, G.; Korobeynikov, A.; Monroe, E. A.; Podell, S.; Glukhov, E.; Allen, E. E.; Gerwick, W. H.; Gerwick, L. Comparative Genomics Uncovers the Prolific and Distinctive

Metabolic Potential of the Cyanobacterial Genus Moorea. *Proc. Natl. Acad. Sci. U.S.A.* **2017**, *114* (12), 3198−3203.

(6) Marquez, B. L.; Watts, K. S.; Yokochi, A.; Roberts, M. A.; Verdier-Pinard, P.; Jimenez, J. I.; Hamel, E.; Scheuer, P. J.; Gerwick, W. H. Structure and Absolute Stereochemistry of Hectochlorin, a Potent Stimulator of Actin Assembly. *J. Nat. Prod.* **2002**, *65* (6), 866−871.

(7) Boudreau, P. D.; Monroe, E. A.; Mehrotra, S.; Desfor, S.; Korobeynikov, A.; Sherman, D. H.; Murray, T. F.; Gerwick, L.; Dorrestein, P. C.; Gerwick, W. H. Expanding the Described Metabolome of the Marine Cyanobacterium Moorea Producens JHB through Orthogonal Natural Products Workflows. *PLoS One* **2015**, *10* (7), No. e0133297.

(8) Edwards, D. J.; Marquez, B. L.; Nogle, L. M.; McPhail, K.; Goeger, D. E.; Roberts, M. A.; Gerwick, W. H. Structure and Biosynthesis of the Jamaicamides, New Mixed Polyketide-Peptide Neurotoxins from the Marine Cyanobacterium Lyngbya Majuscula. *Chem. Biol.* **2004**, *11* (6), 817−833.

(9) Kinnel, R. B.; Esquenazi, E.; Leao, T.; Moss, N.; Mevers, E.; Pereira, A. R.; Monroe, E. A.; Korobeynikov, A.; Murray, T. F.; Sherman, D.; Gerwick, L.; Dorrestein, P. C.; Gerwick, W. H. A Maldiisotopic Approach to Discover Natural Products: Cryptomaldamide, a Hybrid Tripeptide from the Marine Cyanobacterium Moorea Producens. *J. Nat. Prod.* **2017**, *80* (5), 1514−1521.

(10) Oh, D.; Kauffman, C. A.; Jensen, P. R.; Fenical, W. Induced Production of Emericellamides A and B from the Marine-Derived Fungus Emericella sp. in Competing Co-culture. *J. Nat. Prod.* **2007**, *70* (4), 515−520.

(11) Wakefield, J.; Hassan, H. M.; Jaspars, M.; Ebel, R.; Rateb, M. E. Dual Induction of New Microbial Secondary Metabolites by Fungal Bacterial Co-Cultivation. *Front. Microbiol.* **2017**, *8*, 1284.

(12) Wang, M.; Carver, J. J.; Phelan, V. V.; Sanchez, L. M.; Garg, N.; Peng, Y.; Nguyen, D. D.; Watrous, J.; Kapono, C. A.; Luzzatto-Knaan, T.; Porto, C.; Bouslimani, A.; Melnik, A. V.; Meehan, M. J.; Liu, W.-T.; Crüsemann, M.; Boudreau, P. D.; Esquenazi, E.; Sandoval-Calderón, M.; Kersten, R. D.; Pace, L. A.; Quinn, R. A.; Duncan, K. R.; Hsu, C.-C.; Floros, D. J.; Gavilan, R. G.; Kleigrewe, K.; Northen, T.; Dutton, R. J.; Parrot, D.; Carlson, E. E.; Aigle, B.; Michelsen, C. F.; Jelsbak, L.; Sohlenkamp, C.; Pevzner, P.; Edlund, A.; McLean, J.; Piel, J.; Murphy, B. T.; Gerwick, L.; Liaw, C.-C.; Yang, Y.-L.; Humpf, H.-U.; Maansson, M.; Keyzers, R. A.; Sims, A. C.; Johnson, A. R.; Sidebottom, A. M.; Sedio, B. E.; Klitgaard, A.; Larson, C. B.; Boya P, C. A.; Torres-Mendoza, D.; Gonzalez, D. J.; Silva, D. B.; Marques, L. M.; Demarque, D. P.; Pociute, E.; O'Neill, E. C.; Briand, E.; Helfrich, E. J. N.; Granatosky, E. A.; Glukhov, E.; Ryffel, F.; Houson, H.; Mohimani, H.; Kharbush, J. J.; Zeng, Y.; Vorholt, J. A.; Kurita, K. L.; Charusanti, P.; McPhail, K. L.; Nielsen, K. F.; Vuong, L.; Elfeki, M.; Traxler, M. F.; Engene, N.; Koyama, N.; Vining, O. B.; Baric, R.; Silva, R. R.; Mascuch, S. J.; Tomasi, S.; Jenkins, S.; Macherla, V.; Hoffman, T.; Agarwal, V.; Williams, P. G.; Dai, J.; Neupane, R.; Gurr, J.; Rodríguez, A. M. C.; Lamsa, A.; Zhang, C.; Dorrestein, K.; Duggan, B. M.; Almaliti, J.; Allard, P.-M.; Phapale, P.; Nothias, L.-F.; Alexandrov, T.; Litaudon, M.; Wolfender, J.-L.; Kyle, J. E.; Metz, T. O.; Peryea, T.; Nguyen, D.-T.; VanLeer, D.; Shinn, P.; Jadhav, A.; Müller, R.; Waters, K. M.; Shi, W.; Liu, X.; Zhang, L.; Knight, R.; Jensen, P. R.; Palsson, B. Ø.; Pogliano, K.; Linington, R. G.; Gutiérrez, M.; Lopes, N. P.; Gerwick, W. H.; Moore, B. S.; Dorrestein, P. C.; Bandeira, N. Sharing and Community Curation of Mass Spectrometry Data with Global Natural Products Social Molecular Networking. *Nat. Biotechnol.* **2016**, *34* (8), 828−837.

(13) Reher, R.; Kim, H. W.; Zhang, C.; Mao, H. H.; Wang, M.; Nothias, L.-F.; Caraballo-Rodriguez, A. M.; Glukhov, E.; Teke, B.; Leao, T.; Alexander, K. L.; Duggan, B. M.; Van Everbroeck, E. L.; Dorrestein, P. C.; Cottrell, G. W.; Gerwick, W. H. A Convolutional Neural Network-Based Approach for the Rapid Annotation of Molecularly Diverse Natural Products. *J. Am. Chem. Soc.* **2020**, *142* (9), 4114−4120.

(14) Süssmuth, R. D.; Mainz, A. Nonribosomal Peptide Synthesis—Principles and Prospects. *Angew. Chem., Int. Ed.* **2017**, *56* (14), 3770−3821.

(15) Moss, N. A.; Seiler, G.; Leão, T. F.; Castro-Falcón, G.; Gerwick, L.; Hughes, C. C.; Gerwick, W. H. Nature's Combinatorial Biosynthesis Produces Vatiamides A-F. *Angew. Chem., Int. Ed.* **2019**, *58* (27), 9027−9031.

(16) Alonzo, D. A.; Schmeing, T. M. Biosynthesis of Depsipeptides, or Depsi: The Peptides with Varied Generations. *Protein Sci.* **2020**, *29* (12), 2316−2347.

(17) Jumper, J.; Evans, R.; Pritzel, A.; Green, T.; Figurnov, M.; Ronneberger, O.; Tunyasuvunakool, K.; Bates, R.; Žídek, A.; Potapenko, A.; Bridgland, A.; Meyer, C.; Kohl, S. A. A.; Ballard, A. J.; Cowie, A.; Romera-Paredes, B.; Nikolov, S.; Jain, R.; Adler, J.; Back, T.; Petersen, S.; Reiman, D.; Clancy, E.; Zielinski, M.; Steinegger, M.; Pacholska, M.; Berghammer, T.; Bodenstein, S.; Silver, D.; Vinyals, O.; Senior, A. W.; Kavukcuoglu, K.; Kohli, P.; Hassabis, D. Highly Accurate Protein Structure Prediction with AlphaFold. *Nature* **2021**, *596* (7873), 583−589.

(18) Alonzo, D. A.; Chiche-Lapierre, C.; Tarry, M. J.; Wang, J.; Schmeing, T. M. Structural Basis of Keto Acid Utilization in Nonribosomal Depsipeptide Synthesis. *Nat. Chem. Biol.* **2020**, *16* (5), 493−496.

(19) Magarvey, N. A.; Beck, Z. Q.; Golakoti, T.; Ding, Y.; Huber, U.; Hemscheidt, T. K.; Abelson, D.; Moore, R. E.; Sherman, D. H. Biosynthetic Characterization and Chemoenzymatic Assembly of the Cryptophycins. Potent Anticancer Agents from Nostoc Cyanobionts. *ACS Chem. Biol.* **2006**, *1* (12), 766−779.

(20) Ramaswamy, A. V.; Sorrels, C. M.; Gerwick, W. H. Cloning and Biochemical Characterization of the Hectochlorin Biosynthetic Gene Cluster from the Marine Cyanobacterium Lyngbya Majuscula. *J. Nat. Prod.* **2007**, *70* (12), 1977−1986.

(21) Xu, Y.; Kersten, R. D.; Nam, S.-J.; Lu, L.; Al-Suwailem, A. M.; Zheng, H.; Fenical, W.; Dorrestein, P. C.; Moore, B. S.; Qian, P.-Y. Bacterial Biosynthesis and Maturation of the Didemnin Anti-cancer Agents. *J. Am. Chem. Soc.* **2012**, *134* (20), 8625−8632.

(22) Balunas, M. J.; Linington, R. G.; Tidgewell, K.; Fenner, A. M.; Ureña, L. D.; Togna, G. D.; Kyle, D. E.; Gerwick, W. H. Dragonamide E, a Modified Linear Lipopeptide from Lyngbya Majuscula with Antileishmanial Activity. *J. Nat. Prod.* **2010**, *73* (1), 60−66.

(23) Hooper, G. J.; Orjala, J.; Schatzman, R. C.; Gerwick, W. H. Carmabins A and B, New Lipopeptides from the Caribbean Cyanobacterium Lyngbya Majuscula. *J. Nat. Prod.* **1998**, *61* (4), 529−533.

(24) Hindra; Pak, P.; Elliot, M. A. Regulation of a Novel Gene Cluster Involved in Secondary Metabolite Production in Streptomyces Coelicolor. *J. Bacteriol.* **2010**, *192* (19), 4973−4982.

(25) Krause, J.; Handayani, I.; Blin, K.; Kulik, A.; Mast, Y. Disclosing the Potential of the SARP-Type Regulator PapR2 for the Activation of Antibiotic Gene Clusters in Streptomycetes. *Front. Microbiol.* **2020**, *11*, 225.

(26) Ecker, A. K.; Levorse, D. A.; Victor, D. A.; Mitcheltree, M. J. Bioisostere Effects on the EPSA of Common Permeability-Limiting Groups. *ACS Med. Chem. Lett.* **2022**, *13* (6), 964−971.

(27) Moss, N. A.; Leao, T.; Glukhov, E.; Gerwick, L.; Gerwick, W. H. Collection, Culturing, and Genome Analyses of Tropical Marine Filamentous Benthic Cyanobacteria. In *Methods in Enzymology*; Moore, B. S., Ed.; Marine Enzymes and Specialized Metabolism - Part A; Academic Press, 2018; Vol. *604*, pp 3−43.

(28) Wick, R. Rrwick/Filtlong, 2023. https://github.com/rrwick/Filtlong (accessed March 09, 2023).

(29) Wick, R. R.; Judd, L. M.; Gorrie, C. L.; Holt, K. E. Unicycler: Resolving Bacterial Genome Assemblies from Short and Long Sequencing Reads. *PLoS Comput. Biol.* **2017**, *13* (6), No. e1005595.

(30) Kolmogorov, M.; Yuan, J.; Lin, Y.; Pevzner, P. A. Assembly of Long, Error-Prone Reads Using Repeat Graphs. *Nat. Biotechnol.* **2019**, *37* (5), 540−546.

(31) Kang, D. D.; Li, F.; Kirton, E.; Thomas, A.; Egan, R.; An, H.; Wang, Z. MetaBAT 2: An Adaptive Binning Algorithm for Robust and

Efficient Genome Reconstruction from Metagenome Assemblies. *PeerJ* **2019**, *7*, No. e7359.

(32) Parks, D. H.; Imelfort, M.; Skennerton, C. T.; Hugenholtz, P.; Tyson, G. W. CheckM: Assessing the Quality of Microbial Genomes Recovered from Isolates, Single Cells, and Metagenomes. *Genome Res.* **2015**, *25* (7), 1043−1055.

(33) Li, H. *Aligning Sequence Reads, Clone Sequences and Assembly Con*gs with BWA-MEM. Figshare. Poster*, 2014..

(34) Walker, B. J.; Abeel, T.; Shea, T.; Priest, M.; Abouelliel, A.; Sakthikumar, S.; Cuomo, C. A.; Zeng, Q.; Wortman, J.; Young, S. K.; Earl, A. M. Pilon: An Integrated Tool for Comprehensive Microbial Variant Detection and Genome Assembly Improvement. *PLoS One* **2014**, *9* (11), No. e112963.

(35) Manni, M.; Berkeley, M. R.; Seppey, M.; Simão, F. A.; Zdobnov, E. M. BUSCO Update: Novel and Streamlined Workflows along with Broader and Deeper Phylogenetic Coverage for Scoring of Eukaryotic, Prokaryotic, and Viral Genomes. *Mol. Biol. Evol.* **2021**, *38* (10), 4647−4654.

(36) Gurevich, A.; Saveliev, V.; Vyahhi, N.; Tesler, G. QUAST: Quality Assessment Tool for Genome Assemblies. *Bioinformatics* **2013**, *29* (8), 1072−1075.

(37) Blin, K.; Shaw, S.; Kloosterman, A. M.; Charlop-Powers, Z.; van Wezel, G. P.; Medema, M. H.; Weber, T. AntiSMASH 6.0: Improving Cluster Detection and Comparison Capabilities. *Nucleic Acids Res.* **2021**, *49* (W1), W29−W35.

(38) Kautsar, S. A.; Blin, K.; Shaw, S.; Navarro-Muñoz, J. C.; Terlouw, B. R.; van der Hooft, J. J. J.; van Santen, J. A.; Tracanna, V.; Suarez Duran, H. G.; Pascal Andreu, V.; Selem-Mojica, N.; Alanjary, M.; Robinson, S. L.; Lund, G.; Epstein, S. C.; Sisto, A. C.; Charkoudian, L. K.; Collemare, J.; Linington, R. G.; Weber, T.; Medema, M. H. MIBiG 2.0: A Repository for Biosynthetic Gene Clusters of Known Function. *Nucleic Acids Res.* **2019**, *48* (D1), D454−D458.

(39) ESPript 3. https://espript.ibcp.fr/ESPript/ESPript/ (accessed Dec 05, 2022).

(40) *Molecular Operating Environment (MOE)*, 2022.02 Chemical Computing Group ULC, Montreal, QC H3A 2R7, Canada, 2024.

(41) Schrödinger, LLC. *The AxPyMOL Molecular Graphics Plugin for Microsoft PowerPoint*, version 1.8, 2015.

(42) Guinea, J.; Meletiadis, J.; Arikan-Akdagli, S.; Giske, C.; Muehlethaler, K.; Arendrup, M. C. The Subcommittee on Antifungal Susceptibility Testing (AFST) of the ESCMID European Committee for Antimicrobial Susceptibility Testing (EUCAST). Method for the determination of broth dilution minimum inhibitory concentrations of antifungal agents for yeasts. EUCAST Definitive Document E.Def 7.4, 2023.